A versatile Fluorescence Lifetime Imaging System for scanning large areas with high time and spatial resolution

César Bernardo*[a], Etelvina de Matos Gomes[a], Hugo Gonçalves[a], Dmitry Isakov[a], Falk Liebold[b], Eduardo Pereira[a], Vladimiro Pires[a] , Anura Samantilleke[a], Mikhail Vasilevskiy[a], Peter Schellenberg[a]
[a] Center of Physics, University of Minho, Campus de Gualtar, 4710-057 Braga, Portugal;
[b]Analytik Jena AG, D-07745 Jena, Germany

ABSTRACT

We present a flexible fluorescence lifetime imaging device which can be employed to scan large sample areas with a spatial resolution adjustable from many micrometers down to sub-micrometers and a temporal resolution of 20 picoseconds. Several different applications of the system will be presented including protein microarrays analysis, the scanning of historical samples, evaluation of solar cell surfaces and nanocrystalline organic crystals embedded in electrospun polymeric nanofibers. Energy transfer processes within semiconductor quantum dot superstructures as well as between dye probes and graphene layers were also investigated.

Keywords: Fluorescence Lifetime Imaging; Fluorescence microscopy; Laser Scanning Microscopy; Semiconductor quantum dots; Graphene; NLO nano fiber; Solar cells.

1. INTRODUCTION

Fluorescence Lifetime Imaging Microscopy (FLIM) is an imaging technique that consists in obtaining spatially resolved fluorescence decay information. This can often provide information that is unavailable from other microscopy techniques [1-4]. The sensitivity of this technique arises from the dependence of fluorescence decay time on the nanoscopic environment of the molecules probed, which is often much stronger than other parameters such as fluorescence intensity, polarization or emission wavelengths. Additionally the fluorescence intensity depends on the local concentration of the dye probes, while the fluorescence lifetime does not [1]. One major reason for the strong sensitivity of the fluorescence lifetime on the environment is the quenching of dye molecules due to energy transfer to other chromophores in their neighborhood. For example if a pair of interacting proteins or other biomolecules are labeled individually with an donor and an acceptor, respectively, the donor fluorophore will be quenched when the biomolecules labeled with the energy acceptor bind to that labeled with the donor. As quenching represents an additional excitation decay channel, the fluorescence lifetime will be shortened accordingly. The energy transfer process is typically governed by dipolar coupling (Forster mechanism) or direct interaction between the probes (Dexter mechanism). In either case the energy transfer efficiency varies strongly on a sub-nanometer scale with the distance between donor and acceptor molecules. Therefore, this transfer process can be used as a nanoscopic ruler. Other reasons for variations of the fluorescence lifetime may be due to dynamical properties of the environment which alter the rate for radiationless relaxation and correspondingly the lifetime of the excited state. For example, local variations of the microviscosity of the investigated system have been probed by means of the fluorescence lifetime decay [5-8].
While the fluorescence lifetime imaging is the central task, our home-made system is flexibly designed to combine this with standard read-out parameters such as the intensity image and for the spotwise probing of high-resolution spectral (color) information.
The applications of FLIM range from microscopy of biological and medicinally relevant specimens to material science. In section 3 we show specific examples acquired with our system. A particular application in which both high spatial and temporal resolution is simultaneously needed is needed is that of characterizing the fluorescence of mesoscopic sized organic crystals embedded within electropsun polymeric nano-fibers.

*crb@live.com.pt; phone 351 253 604 074; fax 351 253 604 061; www.fisica.uminho.pt

Other applications use the observed variations of the fluorescence lifetime to assess localized modifications associated with, for example the imaging capacity of the retina, or for quality assessments of coatings in solar cell coatings
The system which we have developed overcomes several limitations of commercially available systems. These are typically restricted to smaller scanning areas, due to the dimensions of the microscope or the use of galvano-electrically driven mirrors, which limit the scanning area of the beam. Likewise the time resolution is limited by the pulse width of the laser in the case of pulsed diode lasers, as well as by the use of standard single photon counting photomultipliers which have nanosecond rise times.

2. INSTRUMENTATION

We present an extraordinarily flexible Fluorescence Lifetime Imaging device which can be employed to scan large sample areas with a spatial resolution that can be adjusted from many micrometers down to sub-micrometers and a temporal resolution of 20 picoseconds. Additionally contrast and intensity images can be taken. Furthermore individual coordinates can be addressed to gain spectral information.
A sketch of the system is shown in Figure 1. For excitation, a femtosecond Ti:Sapphire mode-locked laser (Coherent Mira 900F) pumped by a frequency doubled CW Neodymium-laser (Coherent Verdi 5W) is employed. It is tunable in the wavelength range from 700-1000nm and the output can subsequently be frequency doubled (350-500nm) or tripled (270-330nm). The Ti:Sa laser emits a pulse train of 76 million pulses /s with a pulse duration of around 90fs FWHM, which corresponds to a pulse to pulse distance of approximately 13 ns. As typical fluorescence decay times are on this time scale it is often necessary to expand the time span between pulses by employing a pulse picker. Depending on the desired spatial resolution, the laser beam is focused by a lens or a long working length microscope objective to a fixed position while the sample is moved through the focused laser beam by a x-y stage. This allows for measurements of large areas without spatial or time distortion, which is often a problem in systems in which the laser beam is scanned over the sample. For lower spatial resolution a standard lens can be mounted. For the highest resolution imaging a 100X Mitutoyo Plan Infinity-Corrected Long WD Objective mounted to a P.I Instrumente P-721 PIFOC® Piezo Flexure Objective Scanner is employed.

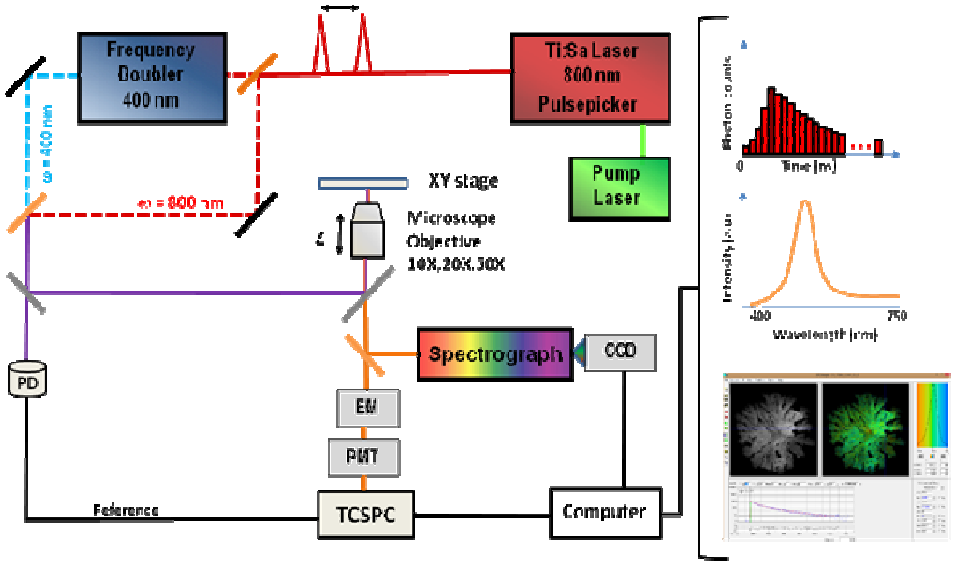

Figure 1. The Fluorescence Lifetime Imaging Microscope consisting of a Ti:Sa mode-locked laser tunable between λ=700–1000 nm and a pulse-picker and a second harmonic generator as excitation source. The sample is scanned through the laser beam by a XY bidirectional motor stage. The single photons are detected by a multi-channel plate photomultiplier and data acquisition is done by a B&H SPC-150 card. Fluorescence intensity images can be taken by using a CCD camera (not shown) and the fluorescence spectra are collected by a 0.3 m monochromator with a CCD detector. A spectrum and a raw data image with a decay curve for one selected point is shown to the right.

The fluorescence decay curves are collected using the Time Correlated Single Photon Counting (TCSPC) technique. A single photon detection Micro-channel plate photomultiplier (MCP), model Hamamatsu R3809U-51 with a temporal resolution of 20 ps is used for detecting the incoming photons. The wavelength selection is achieved by a computer controlled double monochromator (Spectral Products CM-110) or by appropriate filters. The signals are collected by a Time Correlated Single Photon Counting board (Becker&Hickl SPC-150) with a pulse jitter of a few picoseconds. The measurement is done in inverse mode, which means that the start signal to the counter is provided by the fluorescence photon and the stop signal is provided by the delayed trigger signal. The overall time resolution is determined by using a scattering sample and taking the Instrument Response Function (IRF). The overall time-resolution is around 22 ps. For single point measurements or for solution measurements the decay signal is deconvoluted by this IRF. For evaluating images, an approximated IRF is provided for each individual point by calculating the first derivative of the rising part of the experimental kinetics and used for deconvolution.
The sample is mounted on a x-y stage which moves it through the laser beam. This stage is operated by two micro translation DC motors (PI instruments M112.1DG) with a minimal step size of 50 nm and a scanning field of 25x25 mm. However these parameters can be easily adapted by an exchange of the motors without major alteration of the rest of the set-up.
To produce the lifetime image, the card uses three TTL input channels, which indicate the start of a new point measurement, a new line and a new frame, respectively. This was originally designed to be employed with a commercial Laser Scanning Microscope that emits the corresponding TTL signals to communicate the position of the laser beam. We took advantage of this scheme and the TTL for line return and the frame are generated by software through the motor control card. However to provide the necessary precision for individual points within a line, the respective TTL is generated by a timer card (National Instruments NI PCI-6221).
While the main task of the system is to take fluorescence lifetime images, it can also be used to take contrast images and luminescence intensity images by employing a CCD camera. Furthermore individual spots can be addressed and their spectra taken by a glass-fiber coupled monochromator. To this end a 303mm imaging spectrometer (Andor Shamrock SR-303i) with a peltier cooled CCD array (Newton 920) is utilized.

3. APPLICATION EXAMPLES

To demonstrate the versatility of the system several different applications will be presented including protein microarrays analysis, the scanning of historical samples, evaluation of the homogeneity of solar cell surfaces and nanocrystalline organic crystals embedded in electrospun polymeric nanofibers. Energy transfer properties within semiconductor quantum dot superstructures as well as between dye probes and graphene layers have also been investigated.

3.1 Quenching by Graphene

Dye probes or quantum dots in the nanoscale vicinity of graphene crystals show electromagnetic near field coupling to the graphene layer [9;10]. This effect is interesting in its own right but can also be used for energy harvesting [11] or as distance measurements in thin layers. We examined the excited state lifetime of the dye molecules as a function of their distance from the graphene layer. To this end, a series of nanometric polymeric (PMMA) layers were spin-coated on top of pre-identified single layer graphene flakes fixed on glass substrates. PMMA films with thicknesses between 15 and 70nm were obtained by controlling the spinning speed and the concentration of PMMA solved in toluene. These films were then thermally treated before depositing a second sub-nanometer layer of PMMA containing perylene dye molecules. The FLIM set-up was used to measure the fluorescence lifetime of the dye probes in the presence of graphite, few layer graphene, single layer graphene and without an underlying graphene layer for standardization. With this approach we are able to measure distances using an optical microscope, which are orders of magnitude lower than the diffraction limit.

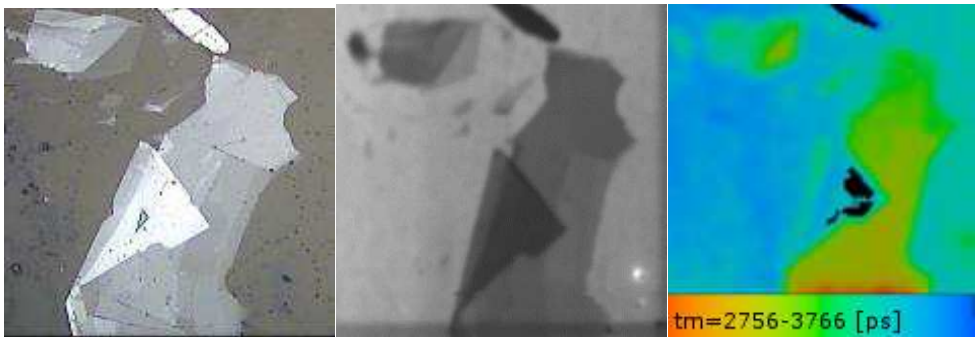

Figure 2. from left to right: reflection microscopy image of a graphitic crystal with monolayer domains. Laser scanning fluorescence intensity image of the same region after spincoating of a 30 nm PMMA layer and a few nm layer of dye doped PMMA ; Fluorescence lifetime image of the same area with color coding of the decay times

3.2 Quantum Nanodot Superstructures

Quantum dots (QDs) are highly efficient luminophores which can be utilized in light reception, building blocks for nano-photonic devices and as sensitizers for solar panels or as biomarkers for bio-imaging applications, just to name a few possibilities [12]. They are extremely photostable, and their wavelength can be tuned throughout the optical spectrum by varying their size, while their other physical and chemical properties remain unmodified.
QDs can aggregate to self-assembled polycrystalline superstructures ranging from nanowires to ordered two-dimensional or three-dimensional superstructures with dimensions in the micrometer range, depending on the ambient conditions during preparation [13;14]. QD nanocrystals also showed interesting energy collection and transfer behavior [15]. Our FLIM set-up has been utilized for fluorescence lifetime imaging as well as spectral mapping of the fluorescence of monodisperse CdSe/ZnS and CdTe QDs dendrite-type fractal superstructures. By this means one can investigate the structural dependence of the energy transfer within these structures [16]. While no spatial variation of the emission spectrum was observed, the fluorescence decay constant was faster in the edges of the dendrite-type superstructures as compared to the center. This has been interpreted as exciton transfer towards the center of the dendrite. The higher QY (Quantum Yield) in CdTe compared to CdSe/ZnS scales with the Quantum efficiency for near–field electromagnetic dipole energy transfer and consequently with a larger Förster radius in these systems. The experimental findings were supplemented by theoretical modeling using master equations for exciton occupation and migration probabilities.
The observed effects may lead to devices with improved energy collection efficiency by using QDs fractal superstructures, for example in light detectors or in solar cell collectors.

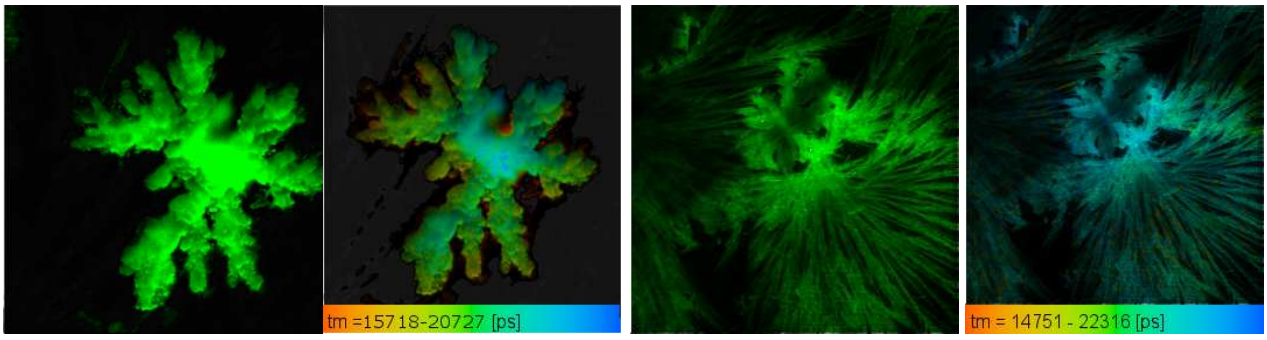

Figure 3. from left to right: Fluorescence image and fluorescence lifetime image of a CdTe dendritic superstructure: The decay time increases from the outer parts of the structure to the center. right: Fluorescence intensity and fluorescence lifetime image of a CdSe/Zns superstructure with a shape that is more filigree. Note that the difference is not due to the chemical composition but rather due to variations in the preparation procedure.

3.3 Electrospun Nanofibers

Electrospun polymer nanofibers of poly-L-lactic acid doped with para-Nitroaniline (p-NA) show an extraordinarily strong second harmonic generation efficiency [17]. This is particularly surprising as bulk crystallites of p-NA consist of unit cells with a centrosymmetic arrangement of the p-NA molecules, which are prohibited from generating second harmonic light by symmetry reasons. It is believed that the unexpectedly strong second harmonic generation in these systems arises from the formation of mesocrystalline structures of *p*-NA which are assembled from nanocrystals with a common orientation, providing surfaces with highly aligned molecules forming a head-to-tail polar arrangement. Centro symmetry is broken the surface allowing second harmonic generation. In this model the individual p-NA molecules in the fiber aggregate and the aligned surfaces generate coherent second harmonic signals which interfere constructively with one another. To qualitatively check this assumption and to evaluate the homogeneity of the doping within the fibers, FLIM experiments have been carried out on layers of these *p*-NA nanofibers as well as on *p*-NA bulk crystals. We were able to show that the fluorescence decay times in the fiber and in a bulk crystal were similar and dramatically shorter than that of *p*-NA in solution. A representative FLIM image is shown in Figure 4.

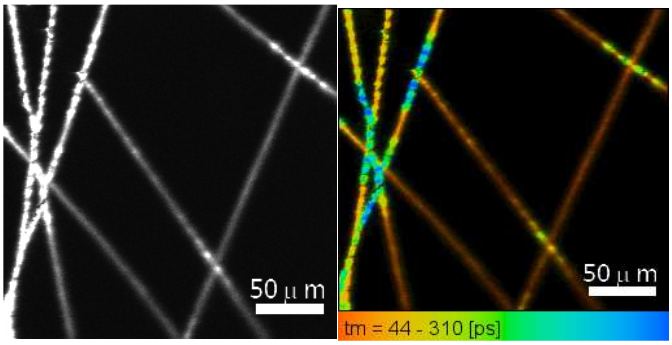

Figure 4. Electrospun polymer nanofibers of poly-L-lactic acid doped with para-Nitroaniline are shown as an intensity image (left) and a color coded lifetime image.

3.4 Solar Cell Surfaces

Photosensitization of wide-band gap nanocrystalline semiconductors by adsorbed dyes is a realistic option for solar cell applications. Dye-sensitized solar cells (DSSC) currently present a promising alternative to conventional solar cells, with power conversion efficiencies as high as 13% having been reported [18]. The fundamental component of the DSSC is a photo-anode consisting of a monolayer of sensitizer dye adsorbed onto a mesoporous semiconductor oxide, typically TiO2. Under operation, dye molecules, adsorbed to the surface of the mesoscopic metal oxide film, inject photogenerated electrons into the conduction band of the metal oxide, which are then transported to an external circuit by diffusion through the TiO_2 film. The oxidized dye cations are then regenerated by electron donation from a redox electrolyte[19] . The sensitizer plays a crucial role not only because it harvests sunlight and generates electric charges, but also because it impairs interfacial charge recombination, being an insulator in the ground state. Polypyridyl ruthenium complexes have proven to be the most efficient sensitizers used in DSSCs to date [18]. Heavy metal-based quantum dots (QDs) have also been identified as efficient sensitizers in QD sensitized solar cells (QDSCs) [20]. Dyes and QDs are also usable as luminescent down-shifting (LDS) materials in solar cells. The incorporation of luminescent down-shifting (LDS) sensitizers into the photoanode of solar cells has the potential to significantly enhance the photocurrent and hence the performance of the cell. An optimized LDS sensitizer consisting of tris (8-quinolinolato) aluminum (Alq3) has already resulted in reasonable enhancement in the conversion efficiency of a number of solar cells [21]. These sensitizers act to harvest primary excitation energy and are expected to transfer it non-radiatively without being quenched. Therefore, in the work carried out in this study, a luminescent decay analysis is carried out to investigate quenching of fluorescence due to the presence of competing non-radiative processes in DSSC and QDSC (Figure 5).

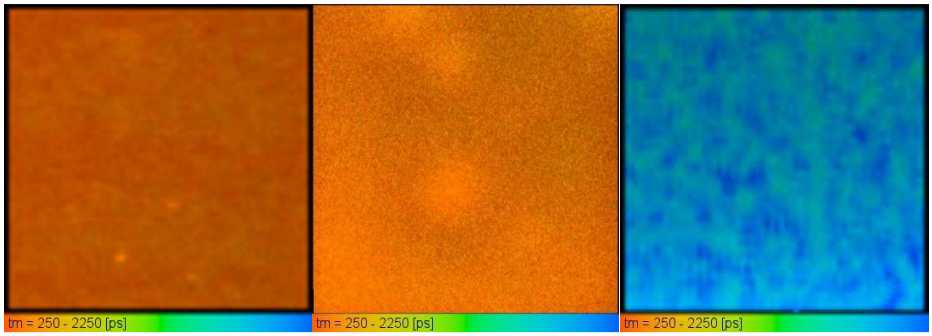

Figure 5. Scan of dye-sensitized solar cell surfaces which are doped with TiO_2 doped with the complex $Ru^{II}(bpy)_2(L^1)$, (with bpy=2,2'-bipyridyl, L^1=4-[2-(4'-methyl-2,2'-bipyridinyl-4-yl)vinyl]benzene-1,2-diol)[20] (left), TiO_2 doped with the dye Alq3 (middle) and a quantum dot sensitized solar cell based on CdSe/ZnS nanodots (right). One can evaluate the homogeneity of the coating and, by scaling with the fluorescence lifetime in solution, get an indication of the efficiency of the transfer process.

3.5 Protein microarray analysis

Protein microarrays are now established as an important analytical tool in biology and biochemistry, for example for establishing the presence or absence of particular proteins of interest and for studying protein interactions [22;23]. Typically probing the luminescence of labels attached to the proteins is used to analyze protein binding in such an assay [24]. However, the obstruction of binding due to the fluorophore marker can be a major problem. Therefore, the use of label-free protein microarray analysis methods is of utmost importance and presents a challenge, which has so far been met only by a few means, such as interferometry, ellipsometry and surface plasmon resonance. These techniques are favorably complemented by the approach presented here. It is based on the fluorescence decay time analysis of the native UV-fluorescence of the proteins' intrinsic amino acids tryptophan and tyrosine, which may be altered by the binding event due to alterations in their environment or due to quenching processes. and sensitivity [25-27]. In principal the same set-up in the low-resolution version was used here, however due to the excitation at 300 nm, all components had to be suitable for UV range.

3.6 Historical Samples

Historical objects are often faint and original painting, letters or other markers may be invisible to the naked eye. Although it may be possible to recover original patterns by chemical means, such a procedure is out of question for valuable historical samples, and a destruction-free approach is mandatory. Fluorescence Lifetime Imaging may be a suitable tool in such cases. The feasibility of such a method has been demonstrated in several examples in the literature [28;29]. Likewise the combination of lifetime imaging with the already demonstrated use of two photon excitation may enhance the specificity of the technique [30;31]. To demonstrate the general practicability of our set-up to investigate such samples we scanned paper with artificial markers made from sodium iodide and from Fe^{2+} -solutions, which were almost invisible to the naked eye but could be easily been seen in the lifetime image (not shown).

4. CONCLUSIONS

We described a particularly flexible but none the less easy to use home -made Laser Scanning system to take Fluorescence Lifetime as well as intensity images. It can also probe spectral information from individually addressable points with high resolution. The system can easily be adapted to two-photon excitation. As the laser beam is static and the sample is scanned through the excitation spot, no time or spatial distortion of the signal takes place. The system can scan samples of macroscopic dimension with microscopic resolution. The time resolution is limited by the laser and the detector employed. In our implementation with a femtosecond excitation source, the limiting equipment is the multichannel-plate PMT detector with a time resolution of 20ps. We utilized the device for multiple experiments which evolved from our directions of research, but it can easily be extended to numerous other applications, where high resolution and / or large scanning areas are required.

ACKNOWLEDGEMENT

This work was financially supported by the European Regional Development Fund (ERDF) through Programa Operacional Factores de Competitividade (COMPETE: FCOMP-01-0124-FEDER-014628) and the Portuguese Fundação para a Ciência e Tecnologia (FCT) through the projects “Functional structuring, inter-particle interaction and energy transfer in ensembles of nanocrystal dots” (PTDC/FIS/113199/2009), Ultra-fast spectroscopy on the dynamics and relaxation of Dirac electrons in graphene” (PTDC/FIS/101434/2008) and “Low dimensional nanostructures for nonlinear optical applications” PTDC/CTmNAN/114269/2009

REFERENCES

[1] Becker, W. "Fluorescence lifetime imaging – techniques and applications," Journal of Microscopy 247, 119-136 (2012).
[2] Becker,W., [Advanced Time-Correlated Single Photon Counting Techniques], Springer, Berlin, Heidelberg, New York, (2005).
[3] Lakowicz,J.R., [Principles of Fluorescence Spectroscopy, 3rd edition], Springer, (2006).
[4] Truong, K. and Ikura, M. "The use of FRET imaging microscopy to detect protein-protein interactions and protein conformational changes in vivo," Current Opinion in Structural Biology 11, 573-578 (2001).
[5] Hungerford, G., Allison, A., McLoskey, D., Kuimova, M. K., Yahioglu, G. and Suhling, K. "Monitoring Sol-to-Gel Transitions via Fluorescence Lifetime Determination Using Viscosity Sensitive Fluorescent Probes," J. Phys. Chem. B 113, 12067-12074 (2009).
[6] Ramadass, R. and Bereiter-Hahn, J. "Excited state photophysical properties of DASPMI in solvents and living cells," Biophys. J. 326A (2007).
[7] Rei, A., Hungerford, G. and Ferreira, M. I. C. "Probing local effects in silica sol-gel media by fluorescence spectroscopy of p-DASPMI," J. Phys. Chem. B 112, 8832-8839 (2008).
[8] Viseu, T. M. R., Hungerford, G., Coelho, A. F. and Ferreira, M. I. C. "Dye-host interactions for local effects recognition in homogeneous and nanostructured media," J. Phys. Chem. B 107, 13300-13312 (2003).
[9] Gaudreau, L., Tielrooij, K. J., Prawiroatmodjo, G. E. D. K., Osmond, J., de Abajo, F. J. G. and Koppens, F. H. L. "Universal Distance-Scaling of Nonradiative Energy Transfer to Graphene," Nano Letters 13, 2030-2035 (2013).
[10] Gomez-Santos, G. and Stauber, T. "Fluorescence quenching in graphene: A fundamental ruler and evidence for transverse plasmons," Physical Review B 84, (2011).
[11] Britnell, L., Ribeiro, R. M., Eckmann, A., Jalil, R., Belle, B. D., Mishchenko, A., Kim, Y. J., Gorbachev, R. V., Georgiou, T., Morozov, S. V., Grigorenko, A. N., Geim, A. K., Casiraghi, C., Neto, A. H. C. and Novoselov, K. S. "Strong Light-Matter Interactions in Heterostructures of Atomically Thin Films," Science 340, 1311-1314 (2013).
[12] Rogach,A.L. ed., [Semiconductor Nanocrystal Quantum Dots: Synthesis, Assembly, Spectroscopy and Applications], Springer, New York, Wien, (2008).
[13] Sukhanova, A., Volkov, Y., Rogach, A. L., Baranov, A. V., Susha, A. S., Klinov, D., Oleinikov, V., Cohen, J. H. M. and Nabiev, I. "Lab-in-a-drop: controlled self-assembly of CdSe/ZnS quantum dots and quantum rods into polycrystalline nanostructures with desired optical properties," Nanotechnology 18, (2007).
[14] Bigioni, T. P., Lin, X. M., Nguyen, T. T., Corwin, E. I., Witten, T. A. and Jaeger, H. M. "Kinetically driven self assembly of highly ordered nanoparticle monolayers," Nature Materials 5, 265-270 (2006).
[15] Sukhanova, A., Baranov, A. V., Perova, T. S., Cohen, J. H. M. and Nabiev, I. "Controlled self-assembly of nanocrystals into polycrystalline fluorescent dendrites with energy-transfer properties," Angewandte Chemie-International Edition 45, 2048-2052 (2006).
[16] Bernardo, C., Moura, I., Fernandez, Y. N., Nunes-Pereira, E. J., Coutinho, P. J. G., Garcia, A. M. F., Schellenberg, P., Belsley, M., Costa, M. F., Stauber, T. and Vasilevskiy, M. I. "Energy Transfer via Exciton Transport in Quantum Dot Based Self-Assembled Fractal Structures," Journal of Physical Chemistry C 118, 4982-4990 (2014).

[17] Isakov, D., Belsley, M., Gomes, E. D., Goncalves, H., Schellenberg, P. and Almeida, B. "Intense optical second harmonic generation from centrosymmetric nanocrystalline para-nitroaniline," Applied Physics Letters accepted for publication, (2014).
[18] Mathew, S., Yella, A., Gao, P., Humphry-Baker, R., Curchod, B. F. E., shari-Astani, N., Tavernelli, I., Rothlisberger, U., Nazeeruddin, M. K. and Gratzel, M. "Dye-sensitized solar cells with 13% efficiency achieved through the molecular engineering of porphyrin sensitizers," Nature Chemistry 6, 242-247 (2014).
[19] Costa, R. D., Lodermeyer, F., Casillas, R. and Guldi, D. M. "Recent advances in multifunctional nanocarbons used in dye-sensitized solar cells," Energy & Environmental Science 7, 1281-1296 (2014).
[20] Algar, W. R., Kim, H., Medintz, I. L. and Hildebrandt, N. "Emerging non-traditional Forster resonance energy transfer configurations with semiconductor quantum dots: Investigations and applications," Coordination Chemistry Reviews 263, 65-85 (2014).
[21] Raupke, A., Albrecht, F., Maibach, J., Behrendt, A., Polywka, A., Heiderhoff, R., Helzel, J., Rabe, T., Johannes, H. H., Kowalsky, W., Mankel, E., Mayer, T., Gorrn, P. and Riedl, T. "Conformal and Highly Luminescent Monolayers of Alq(3) Prepared by Gas-Phase Molecular Layer Deposition," Acs Applied Materials & Interfaces 6, 1193-1199 (2014).
[22] MacBeath, G. and Schreiber, S. L. "Printing proteins as microarrays for high-throughput function determination," Science 289, 1760-1763 (2000).
[23] Stoll, D., Templin, M. F., Bachmann, J. and Joos, T. O. "Protein microarrays: Applications and future challenges," Current Opinion in Drug Discovery & Development 8, 239-252 (2005).
[24] Wiese, R. "Analysis of several fluorescent detector molecules for protein microarray use," Luminescence 18, 25-30 (2003).
[25] Peters, S., Fritzsche, W., Grigaravicius, P., Striebel, H. M., Greulich, K. O. and Schellenberg, P. "Protein Chip analysis by probing time-resolved UV-fluorescence," Proceedings SPIE 6633, 6633-86 (2007).
[26] Schuttpelz, M., Muller, C., Neuweiler, H. and Sauer, M. "UV fluorescence lifetime imaging microscopy: A label-free method for detection and quantification of protein interactions," Analytical Chemistry 78, 663-669 (2006).
[27] Striebel, H. M., Schellenberg, P., Grigaravicius, P. and Greulich, K. O. "Readout of protein microarrays using intrinsic time resolved UV fluorescence for label-free detection," Proteomics 4, 1703-1711 (2004).
[28] Comelli, D., D'Andrea, C., Valentini, G., Cubeddu, R., Colombo, C. and Toniolo, L. "Fluorescence lifetime imaging and spectroscopy as tools for nondestructive analysis of works of art," Applied Optics 43, 2175-2183 (2004).
[29] Nevin, A., Spoto, G. and Anglos, D. "Laser spectroscopies for elemental and molecular analysis in art and archaeology," Applied Physics A-Materials Science & Processing 106, 339-361 (2012).
[30] Cormack, I. G., Loza-Alvarez, P., Sarrado, L., Tomas, S., mat-Roldan, I., Torner, L., Artigas, D., Guitart, J., Pera, J. and Ros, J. "Lost writing uncovered by laser two-photon fluorescence provides a terminus post quem for Roman colonization of Hispania Citerior," Journal of Archaeological Science 34, 1594-1600 (2007).
[31] Nevin, A., Comelli, D., Osticioli, I., Filippidis, G., Melessanaki, K., Valentini, G., Cubeddu, R. and Fotakis, C. "Multi-photon excitation fluorescence and third-harmonic generation microscopy measurements combined with confocal Raman microscopy for the analysis of layered samples of varnished oil films," Applied Physics A-Materials Science & Processing 100, 599-606 (2010).